A&A 416, 235–241 (2004)
DOI: 10.1051/0004-6361:20031708

Astronomy & Astrophysics

Surface C–H stretching features on meteoritic nanodiamonds⋆

A. P. Jones[1], L. B. d'Hendecourt[1], S.-Y. Sheu[2], H.-C. Chang[2], C.-L. Cheng[3], and H. G. M. Hill[4]

[1] Institut d'Astrophysique Spatiale (IAS), Université Paris Sud, Bât. 121, 91405 Orsay Cedex, France
e-mail: Anthony.Jones@ias.u-psud.fr; Louis.DHendecourt@ias.u-psud.fr
[2] Institute of Atomic and Molecular Sciences, Academia Sinica, PO Box 23-116, Taipei, Taiwan 106, ROC
e-mail: alicesys@uchicago.edu; hcchang@po.iams.sinica.edu.tw
[3] Department of Physics, National Dong Hwa University, Hua-Lien, Taiwan 974, ROC
e-mail: clcheng@mail.ndhu.edu.tw
[4] International Space University, Strasbourg Central Campus, Parc d'Innovation, 67400 Illkirch-Graffenstaden, France
e-mail: hill@isu.isunet.edu

Received 14 April 2003 / Accepted 1 December 2003

Abstract. Nanometre-sized diamonds (nanodiamonds) are to date the most abundant presolar grains in primitive meteorites. They are therefore presumed to be an abundant component of the dust in the interstellar medium. What then are the expected spectroscopic signatures of these grains in the interstellar medium? In order to answer this question we have examined the infrared spectroscopic properties of the nanodiamonds extracted from the Orgueil meteorite. The nanodiamonds were surface-cleaned and hydrogenated under vacuum. The spectra of the surface C–H stretching features in the 3–5 μm region were then taken. Comparison with larger synthetic nanodiamonds shows that the spectra are size-dependent. The observed meteoritic nanodiamond C–H stretching features are very different from the features seen on the surfaces of larger diamonds (sizes ≥50 nm). Less-processed Orgueil nanodiamonds appear to provide an intriguing similarity to the class B infrared emission band spectra in the 3.3–3.7 μm wavelength region. The spectra of the nanodiamond C–H stretching features can be used as a template in the search for interstellar nanodiamonds in the infrared spectra of astronomical objects. In addition the size-dependence of the nanodiamond surface C–H features can be used to place rigid and robust constraints upon the sizes of these particles in circumstellar media and in the ISM.

Key words. dust, extinction – circumstellar matter – ISM: individual objects: Elais 1 – ISM: individual objects: HD 97048 – ISM: individual objects: IRAS 05341+0852 – ISM: general

1. Introduction

Presolar diamond nanoparticles (nanodiamonds) were first extracted from primitive meteorites in 1987 (Lewis et al. 1987). Since that time there has been no conclusive evidence for their existence in the interstellar medium but they are expected to be there in quantity. Nanodiamonds are, to date, the most abundant presolar grains, both in terms of mass and number, that have been extracted from primitive meteorites. They have mean sizes of the order of 2–3 nm. It was recently shown (Dai et al. 2002) that some meteoritic nanodiamonds may have been formed in the early solar system. However, the anomalous Xe isotopic composition of the meteoritic nanodiamonds (the so-called Xe-HL component) shows that at least some fraction of them could not have been formed in the solar system (e.g., Anders & Zinner 1993). By inference, therefore, similar diamond nanoparticles should exist in the interstellar medium (ISM) today.

There is perhaps some evidence, from the tentative attribution of an emission band at ~21 μm to diamond, for the presence of nanodiamonds around some protoplanetary nebulae (Hill et al. 1998). A strong ~21 μm band is observed in nitrogen-rich natural diamond and a similar band is seen in neutron-irradiated nitrogen-poor diamond (e.g., Hill et al. 1998). Additionally, the clear observation of diamond surface C–H stretching features in the 3.3–3.6 μm region in two objects (Elias 1 and HD 97048, e.g., Guillois et al. 1999; van Kerckhoven et al. 2002) is strong evidence for the presence of diamond in these circumstellar regions. However, as we shall show in this paper, these observations are *not* consistent with the presence of "true" nanodiamonds in these objects. Indeed the 3.3–3.6 μm spectra of these objects are well-fit by the laboratory spectra of surface C–H features on 50 nm,

Send offprint requests to: A. P. Jones,
e-mail: Anthony.Jones@ias.u-sud.fr
⋆ Appendix A is only available in electronic form at
http://www.edpsciences.org

or larger, diamond particles (Chang et al. 1995; Chen et al. 2002; Sheu et al. 2002). The observed spectra are essentially identical to those for the C–H features on *bulk* diamond crystal surfaces. 50 nm-sized, or larger, diamond particles are therefore bulk-like in their surface structure properties. Nanoparticles, literally taken to be particles with sizes of the order of a nanometre, on the other hand, have very different properties from larger particles and from bulk materials (e.g., Hill et al. 1998). This arises mostly from the fact that a significant fraction of their constituent atoms are in perturbed surface or near-surface states (e.g., Jones 2001). In fact, and on the basis of their unusual properties, it has been suggested that nanodiamonds provide an ideal model for the nature of the very small grains in the interstellar medium (Jones & d'Hendecourt 2000).

In this paper we present the results of our infrared spectroscopic study of meteoritic nanodiamonds, synthetic nanodiamonds and synthetic diamonds. The aim of this study is to elucidate the infrared spectral signatures of the presolar nanodiamonds and to derive observable diagnostics for determining the presence, and the sizes, of the (nano)diamond grains in the ISM. Previous infrared studies of meteoritic nanodiamonds (e.g., Koike et al. 1995; Mutschke et al. 1995; Hill et al. 1997; Andersen et al. 1998) present spectra that are clearly dominated by surface adsorbates introduced during the laboratory extraction process. They are therefore, unfortunately, of little use in the search for interstellar nanodiamonds.

This paper is structured as follows: in Sects. 2 and 3 we describe the experiment and the results. Then, in the following sections, we discuss the measured spectra and the astrophysical consequences (Sect. 4), derive some general (nano)diamond particle diagnostics (Sect. 5) and present our conclusions (Sect. 6).

2. Experiment

The approach adopted in this paper involves two major experimental steps. Firstly, the process of extraction and cleaning of the presolar meteoritic nanodiamonds from a portion of the Orgueil meteorite and, secondly, their subsequent surface cleaning, hydrogenation and infrared spectral analysis.

Throughout the nanodiamond extraction process particular care was taken to extract them under conditions which ensured minimal residual surface contamination. This, in particular, involved a final hydrolysis step that was able to remove almost all of the surface contaminants arising from the extraction process. The nanodiamond extraction was performed using the techniques described in detail elsewhere (Hill et al. 1997; Hill 1998). The identification of the particles as diamond and the sizes were determined by TEM analysis. The extracted nanodiamonds have sizes in the range 1–10 nm, and mean sizes of the order of 2–3 nm. These values are in excellent agreement with other presolar nanodiamond studies (e.g., Daulton et al. 1996; Bernatowicz et al. 1990).

The second step, cleaning, surface hydrogenation and analysis, was undertaken in Taiwan as part of an on-going collaboration between the IAS in Orsay and the Institute of Atomic and Molecular Sciences in Taipei and the Department of Physcis at the National Dong Hwa University, both in Taiwan. The details of the apparatus and the experimental procedure have been published elsewhere (e.g., Chang et al. 1995; Cheng et al. 1997; Chen et al. 2002). Using these same techniques we surface-hydrogenated and analysed the infrared spectra of the presolar nanodiamonds from the Orgueil meteorite, a 5 nm synthetic nanodiamond sample prepared by explosive detonation by Plasmachem GmbH (Mainz, Germany) and 100 nm synthetic diamonds prepared by Kay Industrial Diamond (USA).

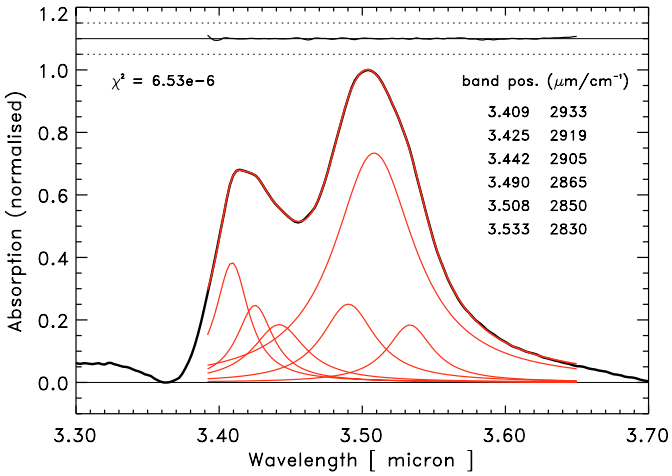

Fig. 1. The Orgueil nanodiamond spectra (2703–3030 cm^{-1}) in the region of the surface C–H stretching features (solid black line) with the Lorentzian profile fits superimposed (grey lines). The mean particle size is ~3 nm. The fit residual (difference + 1.1) is shown in the upper part of the plot along with the χ^2 for the fit. The band positions, in μm and cm^{-1}, are indicated in the tabulated values on the right side of the plot.

Before etching and hydrogenation the (nano)diamonds were annealed to 900 K under vacuum to enable a thorough de-gassing. This step minimises spurious background C–H features. The surface hydrogenation was performed in a hot-filament chemical vapour deposition (HFCVD) reactor providing a constant flow of atomic hydrogen. Subsequent spectral analysis was performed with a Fourier-transform infrared spectrometer (Bomem MB154) at an instrumental resolution of 4 cm^{-1}.

3. Results

The spectroscopic results of this study are presented in Figs. 1 to 3. The hydrogenated, or H-passivated, surfaces of diamond are found to remain stable up to 1200 K, in agreement with the desorption of H from diamond occurring at ~1400 K (e.g., Chen et al. 2002).

Figures 1 to 3 show the 3.3 to 3.7 μm (2703–3030 cm^{-1}) spectra of the three diamond samples that we studied along with Lorentzian band fits to these spectra. We note that for our laboratory spectra Gaussian band fitting profiles may in fact be more appropriate. For spectra taken at high temperatures ($\gg$300 K) vibrational de-phasing can play a significant role in

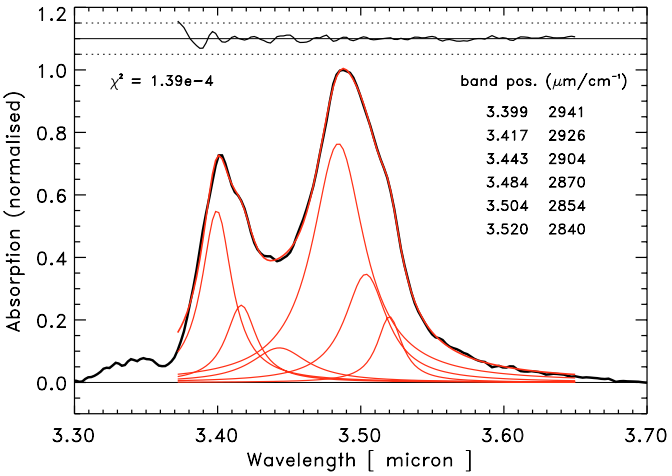

Fig. 2. Same as for Fig. 1 but for the 5 nm synthetic nanodiamond surface C–H stretching features.

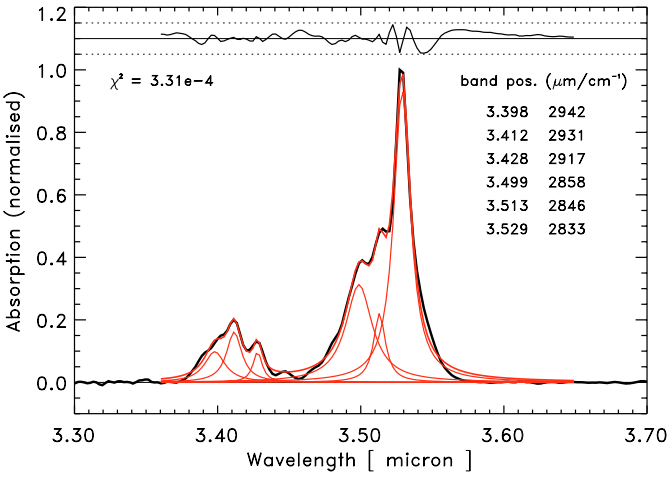

Fig. 3. Same as for Fig. 1 but for the 100 nm synthetic diamond surface C–H stretching features.

Table 1. The Lorentzian band fitting parameters for the (nano)diamond surface C–H stretching vibrations.

Sample	Band position		*FWHM*	Intensity[a]	Band
	μm	cm^{-1}	μm		origin[b]
Orgueil	3.409	2933	0.014	0.520	C{100}
	3.425	2919	0.015	0.328	C{100}
	3.442	2905	0.022	0.254	CH_x
	3.490	2865	0.023	0.329	CH_x
	3.508	2850	0.034	1.000	CH_x
	3.533	2830	0.019	0.252	C{111}
5 nm	3.399	2941	0.013	0.718	C{100}
	3.417	2926	0.013	0.324	C{100}
	3.443	2904	0.024	0.145	CH_x
	3.484	2870	0.022	1.000	CH_x
	3.504	2854	0.018	0.454	CH_x
	3.520	2840	0.010	0.275	C{111}
100 nm	3.398	2942	0.009	0.106	C{100}
	3.412	2931	0.006	0.173	C{100}
	3.428	2917	0.004	0.100	CH_x
	3.499	2858	0.011	0.337	CH_x
	3.513	2846	0.005	0.237	CH_x
	3.529	2833	0.007	1.000	C{111}

[a] N.B. the intensity given here is normalised to that of the strongest band in each (nano)diamond sample.

[b] C{111} (C{100}) indicates C–H stretching on the C{111}-1 × 1 (C{100}) surface, and CH_x (x = 1–3) indicates C–H stretches on corners, edges, defects, etc. (e.g., Chang et al. 1995; Chen et al. 2002).

broadening the absorption bands. In this case the 2833 cm^{-1} band, for example, can be well-fitted with a Lorentzian profile. The spectra reported in this paper were all taken at room temperature where vibrational de-phasing has little effect. The bands are therefore predominantly broadened by the heterogeneous effect due to different surface structures and defects. Here we have used Lorentzian bands to fit our spectra in order to allow some comparison with the results of van Kerckhoven et al. (2002).

For the Lorentzian band fits we used a least squares fitting program to fit a linear baseline-subtracted spectrum. We give the χ^2 for each sample fit in the relevant figure and the full Lorentzian profile fit parameters are presented in Table 1. The band assignments, in Table 1, are taken from Chang et al. (1995). In this work we use six Lorentzian bands to fit the data. This is two profiles less than used by van Kerckhoven et al. (2002) in their match to the observational spectra of the diamond bands in HD 97048 and Elias 1. We use fewer bands because our laboratory data are less well constrained at the shorter wavelengths due to the presence of broad bands in the 3.0 to 3.3 μm region. We do not include the ~3.4 μm band that van Kerckhoven et al. (2002) included in their analysis. The nanodiamond sample spectra show less structure and so we are able to obtain good fits with fewer bands.

We first note that the C–H stretching region displayed here by the Orgueil sample (Fig. 1) is quite different from that obtained by Hill et al. (1997). For example, bands at 3.38, 3.41 and 3.48 μm (2961, 2935 and 2875 cm^{-1}, respectively) were attributed by Hill et al. to CH_2 and CH_3 groups remaining after the chemical extraction process. These bands are certainly not characteristic of clean, hydrogenated diamond surfaces.

Secondly, we notice in the spectra in Figs. 1 to 3, as has already been reported (Chen et al. 2002; Sheu et al. 2002), that as the diamond particle size decreases and approaches nanoparticle (~nm) dimensions, the band sub-structure disappears. In particular, the 3.53 μm band is greatly diminished and is absorbed into the wing of the 3.5 μm band. The 3.53 μm band is attributed to the stretching of sp^3 C–H on the

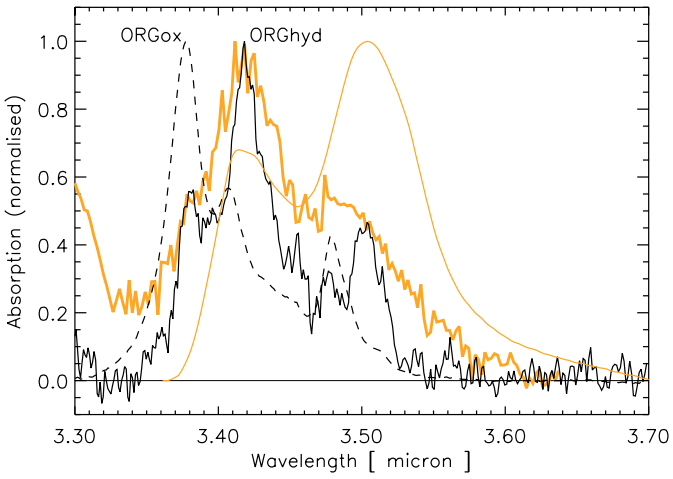

Fig. 4. The Orgueil nanodiamond spectra (2703–3030 cm^{-1}) in the region of the surface C–H stretching features. The smooth grey line is the same spectrum as shown in Fig. 1. The dashed line (continuous black line) shows the further oxidised, ORGox, (hydrolysed, ORGhyd) Orgueil nanodiamond spectra (Hill et al. 1997). A typical class B infrared emission band spectrum, IRAS 05341+0852 (Joblin et al. 1996), is shown for comparison (thick grey line).

well-defined C{111}−1 × 1 surface, and the shorter wavelength bands have been attributed to the stretches of CH_x (x = 1–3) on corners, edges, kinks or other defect sites (Chang et al. 1995; Chen et al. 2002).

In general, for diamond particles smaller than 25 nm (Sheu et al. 2002) the surface C–H 3.3 to 3.7 μm spectra appear as two relatively broad and featureless bands. As Chen et al. (2002) pointed out larger bandwidths are to be expected for oscillators on smaller crystallographic domains. Clearly, as a diamond particle size decreases the given crystal facets must decrease in size. For nanodiamonds there may indeed be no vestiges of well-defined crystal facets and so their spectra must be significantly different. This is the primary effect shown in the spectra in Figs. 1 to 3 (see also Chen et al. 2002; Sheu et al. 2002). The resulting two broad features are a signature of C–H bonds on poorly-defined diamond crystal surfaces. Chen et al. (2002) show that a typical {111} facet on a 4.2 nm diamond contains only a few tens of carbon atoms and is thus too small to prevent severe band broadening. Note that nanodiamond clustering does not affect this fundamental result, i.e., the sharp bands cannot be recovered by clustering into larger aggregates.

The extrapolation of the surface C–H spectroscopic data for diamond particles larger than 50 nm to smaller dimensions is clearly invalid. For nanoparticles the spectra of the surface C–H stretching features are strongly size-dependent and we can therefore use these spectra as a general indicator of the diamond particle size (see Sect. 5).

In Appendix A (available only in the on line version of this article) we show the behaviour of the Lorentzian fit band parameters as a function of the particle size.

3.1. Orgueil nanodiamond spectra: comparison

Here we compare the results of the present study with those presented in our earlier work (Hill et al. 1997). In Fig. 4 we zoom in on the ORGox and ORGhyd data (Hill et al. 1997) in the 3.3 to 3.7 μm (2703–3030 cm^{-1}) region. Note that the features in Fig. 4 are not well-shown in the original data (Fig. 2 of Hill et al. 1997). Unfortunately the longer wavelength data from Hill et al. 1997 either shows little structure (3.6 to 5.6 μm) or is dominated by adsorbed impurities (>5.6 μm) and therefore cannot be used to reveal any useful information on the intrinsic longer wavelength nanodiamond bands.

We note that in Fig. 4 the ORGox data seem to bear little resemblance to the C–H stretching bands of the cleaned and surface-rehydrogenated Orgueil nanodiamonds (Fig. 1). These features are therefore almost certainly due to surface-adsorbed species.

In the ORGhyd data the bands at ~3.42 μm and ~3.50 μm appear to be coincident with the C{100} and CH_x surface C–H stretching features, respectively, in the cleaned and surface-rehydrogenated Orgueil nanodiamonds (see Fig. 1 and Table 1), although, there are clearly some remnants of the bands at ~3.38 μm and ~3.48 μm from the less-processed, oxidised ORGox sample stage.

Figure 4 also shows, for comparison, the observed emission bands in the source IRAS 05341+0852 (Joblin et al. 1996). Interestingly, there appears to be some correspondence between the bands in the ORGox and ORGhyd samples and the observed bands in this source. This will be discussed in more detail in Sect. 4.3.

4. Discussion

The results presented here and elsewhere (Chen et al. 2002; Sheu et al. 2002) clearly show that the spectra of 3–50 nm (nano)diamond particles do not show the distinct 3.43 (2915 cm^{-1}) and 3.53 μm (2835 cm^{-1}) bands. A detailed study of the size-dependent spectra of diamond surface C–H stretching vibrations has been undertaken by Sheu et al. (2002). The results of this study show that the 3.53 μm band is greatly reduced in intensity for sizes smaller than 50 nm and that all well-defined band sub-structure disappears for sizes smaller than 25 nm.

4.1. Diamonds in HD 97048, Elias 1 and HR 4049

Diamonds larger than 50 nm are therefore the only viable explanation for the observed emission bands in HD 97048 and Elias 1, and probably also in HR 4049. This robust conclusion contradicts the sizes of 1–10 nm derived by van Kerckhoven et al. (2002) in their study of these circumstellar diamond emission bands. The diamonds in these sources are consequently not nanodiamonds, are not nanoparticles, and are probably not related to the nanodiamonds extracted from the primitive meteorites Orgueil, Murchison and Allende (sizes ~1–10 nm). This adds weight to the argument that the responsible diamond grains were formed in-situ (van Kerckhoven et al. 2002).

Based on the diamond temperature analysis given by van Kerckhoven et al. (2002) for HD 97048 and Elias 1, we would conclude that diamonds larger than 50 nm would need to be much further from the star than ∼10 AU or that the local FUV radiation field is much weaker than estimated. However, in these calculations (van Kerckhoven et al. 2002) no account was taken of the emission from the diamond bulk and the derived temperatures may therefore need to be revised.

4.2. Substitutional nitrogen in diamonds

We note that the ISO SWS spectra of HD 97048 and Elias 1 show somewhat unusual "7.7" μm bands (van Kerckhoven et al. 2002). In general this band can be decomposed into sub-bands at 7.5, 7.6 and 7.8 μm (Verstraete et al. 2001). In these two sources the 7.8 μm band appears to be the strongest and broadest component. We note that this may be consistent with the diamond interpretation for the 3.43 and 3.53 μm bands because the primary infrared signature of pairs of substitutional nitrogen atoms in diamond (the characteristic spectral signature of type IaA diamond) occurs at ∼7.8 μm (e.g., Davies 1977). Nitrogen atoms are the most abundant substitutional impurities in diamond and could provide a natural explanation for the unusual "7.7" μm bands observed in HD 97048 and Elias 1.

These two sources also show bands in the 20 to 22 μm region (van Kerckhoven et al. 2002). As nitrogen-rich or defective diamonds have been suggested as a source for the ∼21 μm band observed in some protoplanetary nebulae (Hill et al. 1998) this may further add to the case for diamond grains in these two sources.

4.3. Nanodiamonds in the ISM

As we have shown the diamonds in HD 97048 and Elias 1, and probably also in HR 4049, are not the same as the presolar nanodiamonds extracted from primitive meteorites. Thus, the nanodiamonds in the ISM are probably unrelated to the diamonds seen in these sources, at least in terms of the dominant sizes.

In HD 97048 and Elias 1 it is likely that the diamond surfaces would have been "scrubbed" clean by thermal processing at the relatively high temperatures (∼1000 K, van Kerckhoven et al. 2002) that they experience due to their proximity to a star. This would likely be similar to the processing that the (nano)diamonds received in the HFCVD reactor in our experiments. At much higher temperatures (∼2300 K) graphite formation parallel to the C{111} surface occurs (Zhigilei et al. 1997). For nanodiamonds this surface conversion begins at lower temperatures (1400–2000 K, depending on size, Butenko et al. 2000; Braatz et al. 2000).

In the ISM, by comparison, the conditions will be relatively benign and lower temperature surface reactions with carbon and hydrogen can occur. These surface reactions may lead to the formation of a non-diamond (aromatic and aliphatic) carbon components at the surface. In particular, an aromatic component could coordinate perpendicular to the C{111} diamond surface structure in an analogous way to the fundamental role of the graphite/diamond interface in CVD diamond formation and growth (e.g., Lambrecht et al. 1993) as suggested by Jones & d'Hendecourt (2000). Thus, it is not clear that the cleaned and surface-rehydrogenated nanodiamond spectra presented here will necessarily represent the spectra of nanodiamonds in the diffuse ISM. The ISM nanodiamonds may have an important sp^2 carbon component. If such a non-diamond phase was present in our samples it would have been burned away in the HFCVD reactor pre-hydrogenation stage in our experiments.

Perhaps the data shown in Fig. 4 (taken from Hill et al. 1997) may give some clue to the C–H stretching spectral properties of nanodiamonds in the ISM. The ORGox and ORGhyd data both refer to Orgueil nanodiamond samples that have been less processed in the laboratory than the cleaned and surface-rehydrogenated nanodiamonds (Fig. 1). The ORGox and ORGhyd spectra may therefore represent something closer to the spectra of nanodiamonds in the ISM.

Comparison of Fig. 4 with the proposed interstellar IR emission band classification (Geballe 1997) shows that the ORGhyd spectrum is rather similar to the emission band spectrum of the class B source IRAS 05341+0852 (Joblin et al. 1996). Class A are the most common and "typical" IR emission band spectra, class C are the diamond-containing sources (Elias 1 and HD 97048) and the class D spectra are similar to the class B spectra but are only seen in novæ (Geballe 1997). The 3.4 to 3.6 μm spectra of the class B emission band sources show a prominent band at 3.42 μm with a shoulder extending to beyond 3.5 μm (Geballe 1997). Thus, it seems possible that the 3.4 to 3.6 μm spectra in the class B sources, which are rarer than the class A sources, could arise from the emission from nanodiamonds. Interestingly most of the class B sources are also associated with a 21 μm emission feature.

We note that the emission spectrum of the source IRAS 05341+0852 (Joblin et al. 1996) is very reminiscent of the ORGhyd absorption spectrum (Fig. 4). The source IRAS 21282 (van Kerckhoven et al. 2002) also appears to show similarities to the ORGhyd spectrum. The evidence for nanodiamonds in the ISM therefore seems to be somewhat convincing, albeit that the associated sources are rather rare.

5. Diamond and nanodiamond grain size diagnostics

In the light of the work presented here, and by Chen et al. (2002) and Sheu et al. (2002), we can outline a general scheme for determining the size of surface hydrogenated (nano)diamonds from their spectra in the 3.4 to 3.7 μm C–H stretching vibration region. This general diagnostic scheme is presented in Table 2.

To this we may now add that the spectra of 2–3 nm nanodiamonds in the ISM may be more reminiscent of the less laboratory-processed ORGhyd spectrum (Fig. 4). In this case the IR spectrum in the C–H stretching region would show a

Table 2. Diamond and nanodiamond size diagnostics based upon the C–H stretching vibrations in the 3.4 to 3.7 μm spectral region.

Size range	Characteristic spectral features
>50 nm	Broad bands at 3.4 and 3.5 μm with well-defined sub-structure bands at 3.41, 3.43, 3.45, 3.50, 3.51 and 3.53 μm. The 3.53 μm band is particularly strong.
50–25 nm	Broad bands at 3.4 and 3.5 μm with weak sub-structure bands at 3.41, 3.43, 3.45, 3.50, 3.51 and 3.53 μm. Note that the 3.53 μm band now only appears as sub-structure.
25–5 nm	Broad bands at 3.4 and 3.5 μm with a slight asymmetry due to very weak sub-bands in the red wings. There is a clear dip between the two bands.
<5 nm	Broad bands at 3.4 and 3.5 μm with a hint of very weak sub-bands in the red wings. There is a less-pronounced dip between the two bands.

prominent band at ~3.42 μm with a weaker feature, possibly only seen as a shoulder, at ~3.50 μm (e.g., Geballe 1997).

6. Conclusions

We have obtained, for the first time, a spectrum of the C–H stretching bands on "true" natural pre-solar nanodiamonds extracted from the Orgueil meteorite. We show that when the nanodiamond surfaces are appropriately cleaned and re-hydrogenated, the infrared C–H stretching spectral features significantly differ from those presented in earlier laboratory studies. This result is in line with recent studies that show that the infrared spectra of surface hydrogenated diamond particles in the 3.4–3.7 μm (2703–3030 cm^{-1}) wavelength region are strongly size-dependent. Thus, the spectra of the C–H stretches on (nano)diamond surfaces can be used as a robust size diagnostic.

We have shown that the observed 3.43 (2915 cm^{-1}) and 3.53 μm (2835 cm^{-1}) diamonds bands observed in HD 97048 and Elias 1 can only be explained by diamond particles larger than 50 nm.

The requirement that the diamonds in HD 97048 and Elias 1 are not nanodiamonds, but larger particles, now poses some problems for the modelling of these emission bands in these two sources and also for the modelling of the diamond particle temperatures.

Given the discussion presented here it would be worthwhile to search for hydrogenated (nano)diamonds in less extreme circumstellar environments than HD 97048 and Elias 1, e.g., in reflection nebulae and the inner circumstellar shells of proto-planetary nebulae. Additionally, the spectra of nanodiamonds processed under less-extreme conditions than presented here should be obtained. Such an experiment could ascertain if, and what type of, non-diamond structures can exist on their surfaces prior to heating to ~1000 K. In this sense the spectrum of the less-processed Orgueil nanodiamond sample (ORGhyd) may be a useful indicator. This spectrum seems to show that some of the less common interstellar IR emission band spectra could arise from nanodiamond emission.

In the near future we will extend our spectroscopic coverage to longer wavelengths in order to search for other characteristic bands in the nanodiamond spectra. For example, in the two and three phonon region, ~4–5 μm, nanodiamonds look very different from bulk diamond (e.g., Hill et al. 1998).

Acknowledgements. This collaboration has been supported by the CNRS, France. L. d'Hendecourt would like to thank H.-C. Chang and C.-L. Cheng for their hospitality during the course of the collaboration in Taiwan. We thank the anonymous referee for some useful feedback that helped to enhance our discussion. We also thank C. Joblin for providing the data for the source IRAS 05341+0852 as shown in Fig. 4.

References

Anders, E., & Zinner, E. 1993, Meteoritics, 28, 490
Andersen, A. C., Jorgensen, U. G., Nicholaisen, F. M., et al. 1998, A&A, 330, 1080
Bernatowicz, T. J., Gibbons, P. C., & Lewis, R. S. 1990, ApJ, 359, 246
Braatz, A., Banhart, F., & Henning, Th. 2000, Meteoritics & Planetary Science, 34, A16
Butenko, Y., Kuznetsov, V., Chuvilin, A., et al. 2000, J. Appl. Phys., 88, 4380
Chang, H.-C., Lin, J. C., Wu, J. Y., et al. 1995, J. Phys. Chem., 99, 11081
Chen, C.-F., Wu, C.-C., Cheng, C.-L., et al. 2002, J. Chem. Phys., 116, 1211
Cheng, C.-L., Chang, H.-C., Lin, J. C., Song, K.-J., & Wang, J.-K. 1997, Phys. Rev. Lett., 78, 3713
Dai, Z. R., Bradley, J. P., Joswiak, D. J., et al. 2002, Nature, 418, 157
Daulton, T. L., Eisenhour, D. D., Bernatowicz, T. J., et al. 1996, Geochim. Cosmochim. Acta, 60, 4853
Davies, G. 1977, in Chemistry and Physics of Carbon, ed. P. I. Walker, & P. A. Thrower (New York: Marcel Dekker Inc.), 13, 1
Edwards, D. F., & Philipp, H. R. 1985, Handbook of Optical Constants of Solids, ed. E. D. Polik (New York: Academic Press), 665
Geballe, T. R. 1997, in From Stardust to Planetesimals, ed. Y. J. Pendleton, & A. G. G. M. Tielens (SanFrancisco: ASP), ASP Conf. Ser., 122 119
Guillois, O., Ledoux, G., & Reynaud, C. 1999, ApJ, 521, L133
Hill, H. G. M., d'Hendecourt, L. B., Perron, C., et al. 1997, Meteoritics and Planetary Science, 32, 713
Hill, H. G. M. 1998, Ph.D. Thesis, Muséum National d'Histoire Naturelle, Paris
Hill, H. G. M., Jones, A. P., & d'Hendecourt, L. B. 1998, A&A, 336, L41
Joblin, C., Tielens, A. G. G. M., Allamandola, L. J., & Geballe, T. R. 1996, ApJ, 458, 610

Jones, A. P., & d'Hendecourt, L. B. 2000, A&A, 355, 1191
Jones, A. P. 2001, in Galactic Structure, Stars and the Interstellar Medium, ed. C. E. Woodward, M. D. Bicay, & J. M. Shull, ASP Conf. Ser., 231, 171
Koike, C., Wickramasinghe, N. C., Kano, N., et al. 1995, MNRAS, 277, 986
Lambrecht, W. R. L., Lee, C. H., Segall, B., et al. 1993, Nature, 364, 607
Lewis, R. S., Anders, E., & Draine, B. T. 1989, Nature, 339, 117
Lewis, R. S., Tang, M., Wacker, J. F., et al. 1987, Nature, 326, 160
Mutschke, H., Dorschner, J., Henning, T., et al. 1995, ApJ, 454, L157
Sheu, S.-Y., Lee, I.-P., Lee, Y. T., & Chang, H.-C. 2002, ApJ, 581, 55
van Kerckhoven, C., Tielens, A. G. G. M., & Waelkens, C. 2002, A&A, 384, 568
Verstraete, L., Pech, C., Moutou, C., et al. 2001, A&A, 372, 981
Zhigilei, L.V., Srivastava, D., & Garrison, B. J. 1997, Phys. Rev. B, 55, 1838

Online Material

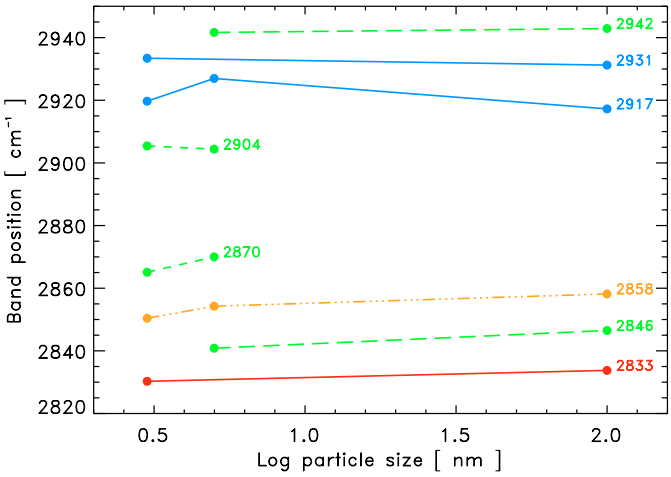

Fig. A.1. Central wavelengths of the Lorentzian bands fitted to the surface C–H stretching features as a function of particle size. The individual plots are labelled by the band positions (in cm^{-1}) of the 100 nm or 5 nm diamond samples (see Table 1).

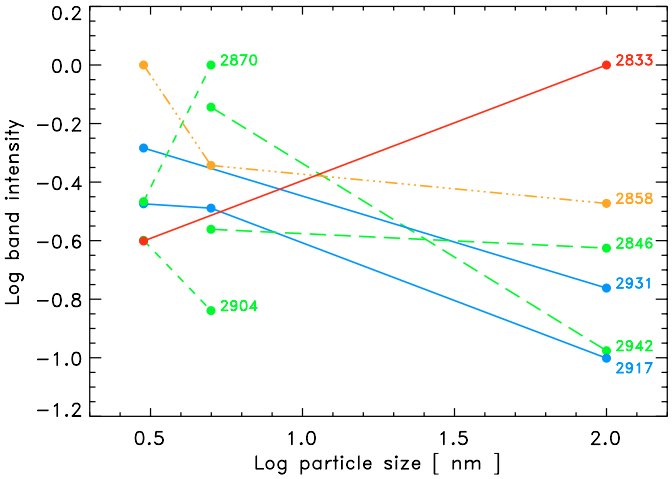

Fig. A.3. Relative intensities (normalised to the strongest band for each sample) of the Lorentzian bands fitted to the surface C–H stretching features as a function of particle size. The bands are indicated as per Fig. A.1.

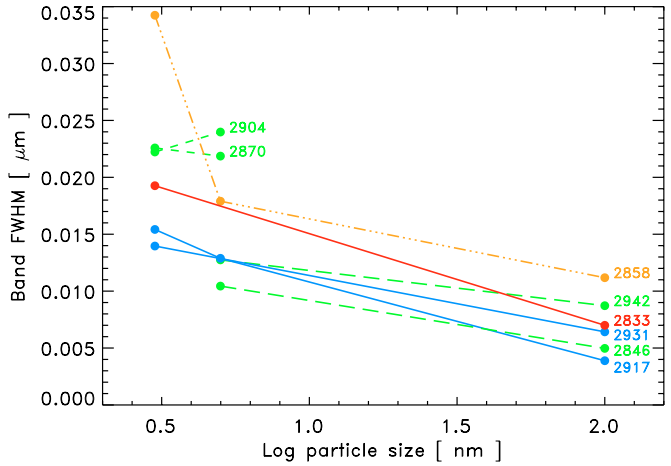

Fig. A.2. *FWHM* of the Lorentzian bands fitted to the surface C–H stretching features as a function of particle size. The bands are indicated as per Fig. A.1.

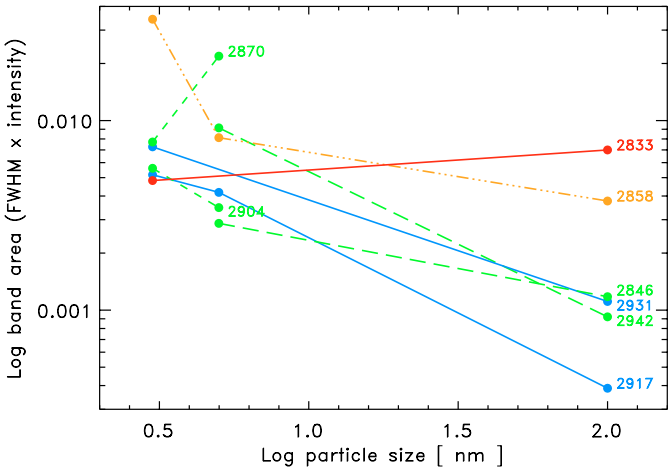

Fig. A.4. Areas (*FWHM* × normalised intensity) of the Lorentzain bands fitted to the surface C–H stretching features as a function of particle size. The bands are indicated as per Fig. A.1.

Appendix A:

In Fig. A.1 we show the fitted band positions as a function of the particle size. Clearly the band shifts as a function of size are less than about 0.01 μm (~10 cm^{-1}). However, in Fig. A.2 we see that the band widths generally decrease with increasing particle size as expected (e.g., Chen et al. 2002). Figure A.3 illustrates how the 3.53 μm (2833 cm^{-1}) band decreases in strength with decreasing particle size. This band is replaced by the 3.5 μm (2830–2860 cm^{-1}) band group as the particle size decreases.

Figure A.4 shows a measure of the integrated band areas as represented by the *FWHM* × normalised intensity. We use this as a measure of the integrated band area, rather than the actual integrated area, because we do not fit the entire spectral range of our plotted data (Figs. 1 to 3). Figure A.4 indicates that the band area generally increases as the particle size decreases, except for the 3.48 and 3.53 μm (2870 and 2833 cm^{-1}, respectively) bands which appear to be absorbed into the other broader bands. These trends are in agreement with the results of Chen et al. (2002) and Sheu et al. (2002).